

# Olanzapine Activates Hepatic Mammalian Target of Rapamycin: New Mechanistic Insight into Metabolic Dysregulation with Atypical Antipsychotic Drugs

Robin H. Schmidt, Jenny D. Jokinen, Veronica L. Massey, K. Cameron Falkner, Xue Shi, Xinmin Yin, Xiang Zhang, Juliane I. Beier, and Gavin E. Arteel

Department of Pharmacology and Toxicology (R.H.S., J.D.J., V.L.M., J.I.B., G.E.A.), and Department of Medicine (K.C.F.), Health Sciences Center, and Department of Chemistry (X.S., X.Y., X.Z.), University of Louisville, Louisville, Kentucky

Received June 28, 2013; accepted August 5, 2013

## ABSTRACT

Olanzapine (OLZ), an effective treatment of schizophrenia and other disorders, causes weight gain and metabolic syndrome. Most studies to date have focused on the potential effects of OLZ on the central nervous system's mediation of weight; however, peripheral changes in liver or other key metabolic organs may also play a role in the systemic effects of OLZ. Thus, the purpose of this study was to investigate the effects of OLZ on hepatic metabolism in a mouse model of OLZ exposure. Female C57Bl/6J mice were administered OLZ (8 mg/kg per day) or vehicle subcutaneously by osmotic minipumps for 28 days. Liver and plasma were taken at sacrifice for biochemical analyses and for comprehensive two-dimensional gas chromatography coupled to time-of-flight mass spectrometry metabolomics analysis. OLZ increased body weight, fat pad mass, and liver-to-body weight ratio without commensurate increase in

food consumption, indicating that OLZ altered energy expenditure. Expression and biochemical analyses indicated that OLZ induced anaerobic glycolysis and caused a pseudo-fasted state, which depleted hepatic glycogen reserves. OLZ caused similar effects in cultured HepG2 cells, as determined by Seahorse analysis. Metabolomic analysis indicated that OLZ increased hepatic concentrations of amino acids that can alter metabolism via the mTOR pathway; indeed, hepatic mTOR signaling was robustly increased by OLZ. Interestingly, OLZ concomitantly activated AMP-activated protein kinase (AMPK) signaling. Taken together, these data suggest that disturbances in glucose and lipid metabolism caused by OLZ in liver may be mediated, at least in part, via simultaneous activation of both catabolic (AMPK) and anabolic (mammalian target of rapamycin) pathways, which yields new insight into the metabolic side effects of this drug.

## Introduction

Olanzapine (OLZ) is one of the most effective drug options for managing the symptoms of schizophrenia and bipolar disorder (Lee et al., 2002). Unlike the first-generation antipsychotic medications (e.g., haloperidol), the risk of tardive dyskinesia is low with OLZ, and acute idiosyncratic toxicity is rare. These attributes make OLZ a drug of choice to treat severe mental illness. Indeed, the lack of severe side effects has expanded the off-label use of the drug for indications such as dementia and treatment-resistant anxiety disorders (Maher and Theodore, 2012). Although OLZ does not share the severe toxicity of its first-generation predecessors, it does have side

effects that limit its therapeutic potential. Numerous studies show that OLZ causes substantial weight gain only weeks after the start of administration, and that this weight gain persists throughout treatment (Mathews and Muzina, 2007). These effects strongly negatively influence patient treatment compliance (Weiden et al., 2004).

OLZ-induced weight gain is not only an issue for patient compliance, but can also induce sequelae associated with weight gain/obesity such as glucose intolerance and/or insulin resistance. Interestingly, the changes induced by OLZ administration in carbohydrate and lipid metabolism may in fact precede weight gain, which suggests a potential direct effect of the drug on these pathways (Chintoh et al., 2008). The side effects of OLZ on weight gain and glucose metabolism are particularly relevant at this time, with obesity increasing at an alarming rate in the United States and other industrialized countries (Ogden et al., 2006). Moreover, even within an increasingly overweight general population, obesity

This work was supported in part by the National Institutes of Health National Institute of General Medical Sciences [Grant GM087735]; and by the National Institutes of Health National Institute of Environmental Health Sciences [Grant T32-ES011564] (Predoctoral Fellowship to R.H.S. and V.L.M.).  
dx.doi.org/10.1124/jpet.113.207621.

**ABBREVIATIONS:** Akt, protein kinase B; AMPK, AMP-activated protein kinase; CNS, central nervous system; 4EBP1, eukaryotic translation initiation factor 4E-binding protein 1; FCCP, carbonyl cyanide 4-(trifluoromethoxy)phenylhydrazone; GC×GC-TOF-MS, comprehensive two-dimensional gas chromatography coupled to time-of-flight mass spectrometry; HDL, high-density lipoprotein; LDL, low-density lipoprotein; MTBSTFA, *N*-(*tert*-butyldimethylsilyl)-*N*-methyltrifluoroacetamide; mTOR, mammalian target of rapamycin; NEFA, nonesterified fatty acids; OCR, oxygen consumption rate; OGTT, oral glucose tolerance test; OLZ, olanzapine; p70S6K, 70-kDa ribosomal protein S6 kinase; PAS, periodic acid-Schiff; PPR, proton production rate; RT-PCR, reverse transcription-polymerase chain reaction; TBDMSCI, *tert*-butyldimethylchlorosilane; TG, triglycerides; VLDL, very-low-density lipoprotein.

disproportionately affects individuals with severe mental illnesses (Allison et al., 2009). Therefore, it is necessary to develop strategies that prevent, minimize, or reverse the adverse metabolic effects that occur during OLZ treatment, especially for a population already at risk for obesity and its sequelae (Heiskanen et al., 2003).

The beneficial effects of OLZ are assumed to be mediated at the level of the central nervous system (CNS). Not surprisingly, most studies into the metabolic side effects of OLZ have also focused on the CNS (Weston-Green et al., 2012). Although the CNS clearly plays a key role in regulating food consumption, obesity, dyslipidemia, and diabetes (Sandoval et al., 2009; Grayson et al., 2013), peripheral organs also significantly contribute to metabolic dysregulation in the intact organism. To date, very little is understood about the potential effects of OLZ administration on the peripheral organs critical for metabolic homeostasis. The liver is key for overall glucose and lipid homeostasis, and recent studies have suggested that the effect of OLZ on the liver may contribute to its metabolic disturbances (Girault et al., 2012). Therefore, we explored the effects of OLZ on indices of carbohydrate and lipid metabolism in this organ and determined the underlying mechanisms in a mouse model of OLZ exposure.

## Materials and Methods

**Animals and Treatments.** Female C57BL/6J mice (8 weeks old) were purchased from The Jackson Laboratory (Bar Harbor, ME). The mice were housed in a pathogen-free barrier facility accredited by the Association for Assessment and Accreditation of Laboratory Animal Care, and the procedures were approved by the University of Louisville Institutional Animal Care and Use Committee. Food and tap water were allowed ad libitum. One week before the initiation of the experiment, the animals were switched from standard chow to purified TD.08485 diet (Harlan Laboratories, Madison, WI) to avoid any batch-to-batch variability in the food content (see Fig. 1A). Olanzapine (8 mg/kg per day; Kapur et al., 2003) or vehicle (saline) was given subcutaneously via osmotic minipumps (Alzet, Cupertino, CA) for 28 days. To avoid concerns of OLZ degradation, the pumps were replaced after 2 weeks (van der Zwaal et al., 2008). The animals were weighed on a weekly basis, and their food consumption was recorded twice per week. After 28 days, the mice were anesthetized with ketamine/xylazine (100/15 mg/kg i.p.), and the minipumps were removed. Body composition was assessed by dual-energy X-ray absorptiometry (DEXA) using a Lunar PIXImus densitometer (Lunar Corp., Madison, WI) according to the manufacturer's instructions. Blood was collected from the vena cava just before sacrifice by exsanguination, and citrated plasma was stored at  $-80^{\circ}\text{C}$  for further analysis. Portions of liver tissue were frozen immediately in liquid nitrogen, fixed in 10% neutral buffered formalin, or frozen-fixed for subsequent sectioning and mounting on microscope slides. Blood, liver, and gonadal fat pads were collected for later analysis.

**Oral Glucose Tolerance Test.** An oral glucose tolerance test (OGTT) (Andrikopoulos et al., 2008) was performed after 25 days of OLZ exposure. In brief, mice were transferred to cages that had been cleared of food and bedding, and they were fasted for 6 hours. Blood was sampled from the tail vein immediately after the fasting period, and then 15, 30, 60, 90, and 120 minutes after oral administration of 2 mg/kg D-(+)-glucose (Sigma-Aldrich, St. Louis, MO) in sterile saline (4 ml/kg) solution. Glucose concentrations were measured using an Accu-Chek Aviva Plus glucometer and test strips (Roche Diagnostics Corp., Indianapolis, IN).

**Biochemical Analyses and Histology.** Plasma levels of alanine aminotransferase (ALT), aspartate aminotransferase (AST), total cholesterol, high-density lipoprotein (HDL), low-density lipoprotein

(LDL), very-low-density lipoprotein (VLDL), triglycerides (TG), and glucose were determined by the Piccolo Lipid Panel Plus Reagent Disc, used with the Piccolo Xpress Chemistry Analyzer (Abaxis, Inc., Union City, CA), according to the manufacturer's instructions. Paraffin-embedded sections of liver were stained with hematoxylin and eosin (H&E) to assess overall hepatic structure. Hepatic lipids—TG and nonesterified fatty acids (NEFA)—were extracted in chloroform/methanol (Bligh and Dyer, 1959) and measured as described previously elsewhere (Bergheim et al., 2006). Results were normalized to the wet weight of extracted tissue.

For detection of hepatic neutral lipids in tissue, 10- $\mu\text{m}$  frozen sections were stained with Oil Red O (Sigma-Aldrich) for 10 minutes, washed, and counterstained with hematoxylin for 45 seconds (Bergheim et al., 2006). For hepatic glycogen staining, paraffin sections (5  $\mu\text{m}$ ) were deparaffinized and rehydrated, oxidized in 0.5% periodic acid solution for 5 minutes, washed, placed in Schiff reagent for 15 minutes, washed, and counterstained with hematoxylin for 1 minute. Staining was quantitated by image analysis, as described previously elsewhere (Bergheim et al., 2006).

**RNA Isolation and Real-Time Reverse Transcription-Polymerase Chain Reaction.** RNA extraction and real-time reverse transcription-polymerase chain reaction (RT-PCR) were performed as described previously elsewhere (Bergheim et al., 2006). The PCR primers and probes were purchased premade from Applied Biosystems (Carlsbad, CA) and were designed to span introns to avoid amplification of any contaminating DNA. The comparative  $C_t$  method was used to determine fold differences between samples and the calibrator gene ( $\beta$ -actin), and the purity of PCR products was verified by gel electrophoresis. The comparative  $C_t$  method determines the amount of target, normalized to an endogenous reference ( $\beta$ -actin) and relative to a calibrator ( $2^{\Delta\Delta C_t}$ ).

**Immunoblots.** Frozen liver samples were homogenized in radioimmunoprecipitation assay buffer (20 mM Tris, pH 7.4, 150 mM NaCl, 1 mM EDTA, 1 mM EGTA, 1 mM  $\beta$ -glycerophosphate, 1 mM  $\text{Na}_3\text{VO}_4$ , and 1% w/w Triton X-100) containing protease, tyrosine/phosphatase, and serine/threonine phosphatase inhibitor cocktails (Sigma-Aldrich). Lysates were sonicated and subsequently centrifuged for 5 minutes at 16,000g. The protein concentration of the supernatants was determined with the Bio-Rad DC Protein Assay (Bio-Rad Laboratories, Hercules, CA); 100  $\mu\text{g}$  of total protein were mixed with 4 $\times$  sample loading buffer (250 mM Tris, pH 7.4, 10% SDS, 20% 2-mercaptoethanol, 40% glycerol, and 0.01% w/v bromophenol blue) and incubated at  $95^{\circ}\text{C}$  for 5 minutes. The samples were loaded onto SDS-polyacrylamide gels (Bio-Rad Laboratories), followed by electrophoresis and Western blotting onto polyvinylidene difluoride membranes (Hybond P; Amersham Biosciences, Piscataway, NJ). Antibodies against AMP-activated protein kinase  $\alpha$  (AMPK $\alpha$ ), phospho-AMPK $\alpha$  (p-AMPK $\alpha$ ), protein kinase B (Akt), phospho-Akt (p-Akt), mammalian target of rapamycin (mTOR), phospho-mTOR (p-mTOR), 70-kDa ribosomal protein S6 kinase (p70S6K) (Bethyl Laboratories, Montgomery, TX), phospho-p70S6K (p-p70S6K), eukaryotic translation initiation factor 4E-binding protein 1 (4EBP1) (Bethyl Laboratories), and phospho-4EBP1 (p-4EBP1) were used at the dilutions recommended by the suppliers (Cell Signaling Technology, Danvers, MA; unless otherwise indicated). Horseradish peroxidase-coupled secondary antibodies and chemiluminescence detection reagents were obtained from Pierce (Rockford, IL). The signals were detected using Classic Blue autoradiography film BX (MIDSCI, St. Louis, MO). Densitometric quantitation was performed with UN-SCAN IT analysis software (Silk Scientific, Orem, UT), as described previously elsewhere (Bergheim et al., 2006).

**Bioenergetic Measurements (HepG2 Cells).** Bioenergetic measurements were made using an XF96 Extracellular Flux Analyzer (Seahorse Biosciences, Billerica, MA). HepG2 cells (American Type Culture Collection, Manassas, VA) were plated at 10,000 cells per well and grown for 24 hours in Dulbecco's modified Eagle's medium (Invitrogen, Carlsbad, CA) containing either glucose (25 mM) or galactose (10 mM) and 6 mM pyruvate. Immortalized cells preferentially use anaerobic glycolysis to meet energy demands, even in the

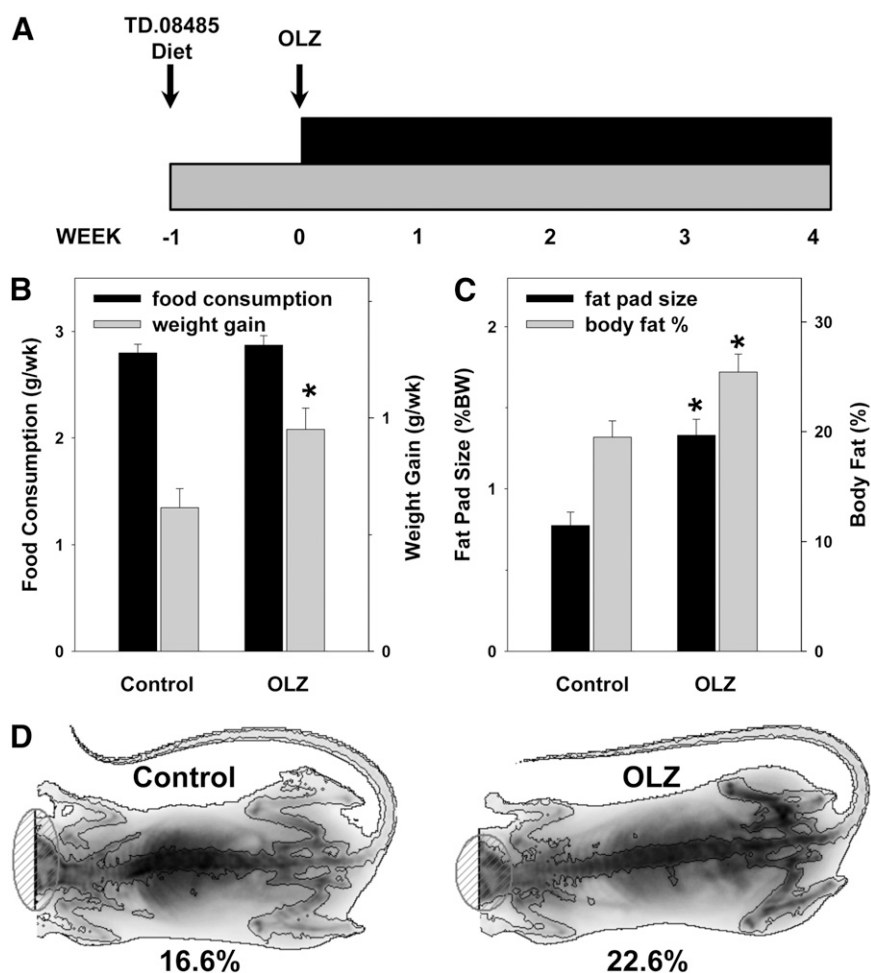


**Fig. 1.** Effect of OLZ on body weight gain and adiposity. (A) Schematic of the experimental design. (B) Average weekly food consumption and weight gain. (C) Fat pad and total body fat. (D) Representative dual-energy X-ray absorptiometry (DEXA) scan images. Low-density areas depict soft matter (i.e., body fat). \* $P < 0.05$  compared with controls.

presence of adequate oxygen (Warburg et al., 1967). Anaerobic glycolysis of galactose yields no net ATP and forces cells to rely on oxidative phosphorylation (Marroquin et al., 2007). Cells were then treated with graded concentrations of olanzapine from 0 to 25  $\mu\text{M}$ . One hour before the commencement of measurements, the medium was changed to unbuffered Dulbecco's modified Eagle's medium (Seahorse Biosciences) containing the same concentrations of sugars, pyruvate, or olanzapine. The XF96 Extracellular Flux analyzer measures the OCR (oxygen consumption rate) and PPR (proton production rate) in a small transient chamber in specialized plates. Seeding density was optimized under the cell culture conditions described to ensure linear oxygen consumption and adequate mixing during the re-equilibration phases. Coupled and uncoupled OCR and PPR measurements were made by addition of oligomycin (1  $\mu\text{g}/\text{ml}$ ) and carbonyl cyanide 4-(trifluoromethoxy)phenylhydrazone (FCCP; 1  $\mu\text{M}$ ), respectively, through sequential injections from ports in the Seahorse Flux Pak cartridges.

**Metabolite Sample Preparation.** A sample of liver tissue was weighed and homogenized for 2 minutes after adding water at a concentration of 100 mg/ml. The homogenized sample was then stored at  $-80^{\circ}\text{C}$  until use. A 100- $\mu\text{l}$  aliquot of the homogenized liver sample and 400  $\mu\text{l}$  of ice-cold methanol were mixed and vortexed for 2 minutes and then incubated for 10 minutes on ice followed by another 2-minute vortex. The mixtures were centrifuged at  $4^{\circ}\text{C}$  for 10 minutes at 15,000g. We aspirated 400  $\mu\text{l}$  of the supernatant into a microcentrifuge tube, which was then dried overnight in a centrifugal evaporator (SpeedVac; Thermo-Fisher, Waltham, MA). The extracted metabolites were then dissolved in 40  $\mu\text{l}$  of acetonitrile. After adding 40  $\mu\text{l}$  of *N*-(*tert*-butyldimethylsilyl)-*N*-methyltrifluoroacetamide (MTBSTFA) mixed with 1% *tert*-butyldimethylchlorosilane (TBDMSCI), the mixture was

sonicated for 3 hours followed by overnight derivatization at room temperature. The samples were then transferred to gas chromatography vials for analysis. The derivatization was performed just before comprehensive two-dimensional gas chromatography coupled to time-of-flight mass spectrometry (GC $\times$ GC-TOF-MS) analysis.

**GC $\times$ GC-TOF-MS Analysis.** The LECO Pegasus 4D GC $\times$ GC-TOF-MS instrument was equipped with an Agilent 6890 gas chromatograph and a Gerstel MPS2 autosampler (GERSTEL, Inc., Linthicum, MD), featuring a LECO two-stage cryogenic modulator and secondary oven. The primary column was a 60 m  $\times$  0.25 mm  $^{\text{t}}d_c \times$  0.25  $\mu\text{m}^{\text{t}}d_f$  DB-5ms GC capillary column [phenyl arylene polymer virtually equivalent to (5%-phenyl)-methylpolysiloxane]. A second GC column of 1 m  $\times$  0.25 mm  $^{\text{t}}d_c \times$  0.25  $\mu\text{m}^{\text{t}}d_f$  DB17ms [(50% phenyl)-methylpolysiloxane] was placed inside the secondary GC oven after the thermal modulator. Both columns were obtained from Agilent Technologies (Santa Clara, CA).

The helium carrier gas (99.999% purity) flow rate was set to 2.0 ml/min at a corrected constant flow via pressure ramps. The inlet temperature was set at  $280^{\circ}\text{C}$ . The primary column temperature was programmed with an initial temperature of  $60^{\circ}\text{C}$  for 0.5 minutes and then was ramped at  $5^{\circ}\text{C}$  per minute to  $270^{\circ}\text{C}$  and kept for 15 minutes. The secondary column temperature program was set to an initial temperature of  $70^{\circ}\text{C}$  for 0.5 minutes and then also ramped at the same temperature gradient used in the first column to  $280^{\circ}\text{C}$  accordingly. The thermal modulator was set to  $+15^{\circ}\text{C}$  relative to the primary oven, and a modulation time of  $P_M = 2$  second was used. The mass range was set as 29–800  $m/z$  with an acquisition rate of 200 mass spectra per second. The ion source chamber was set at  $230^{\circ}\text{C}$  with the transfer line temperature set to  $280^{\circ}\text{C}$ , and the detector voltage was 1450 V

with electron energy of 70 eV. The acceleration voltage was turned on after a solvent delay of 674 second. The split ratio was set at 25:1.

**GC×GC-TOF MS Data Analysis.** The GC×GC-TOF MS data were processed using LECO's instrument control software (ChromatOF) for peak picking and tentative metabolite identification, followed by retention index matching, peak merging, peak list alignment, normalization, and statistical significance test using MetPP software (Wei et al., 2013). For metabolite identification using ChromaTOF, each chromatographic peak was tentatively assigned to a metabolite if its experimental mass spectrum and a database spectrum have a spectral similarity score no less than 600. The retention index matching in MetPP was performed using the iMatch method with the  $P$  value threshold set as  $P \leq 0.001$  (Zhang et al., 2011). The pairwise two-tail  $t$  test was used to determine whether a metabolite had a statistically significant abundance difference between sample groups by setting the threshold of false discovery rate  $q \leq 0.3$ .

Functional clustering, enrichment and pathway analysis of the regulated metabolites was performed using the Metacore (Thomson Reuters, <http://www.genego.com/metacore.php>) platform, according to the site's instructions. Through this platform, metabolites were analyzed using the map folders, pathway maps, process networks, and metabolic networks enrichment analysis. Final networks were

transferred to Pathway Map Creator tool (Thomson Reuters) to create a signaling map.

**Statistical Analysis.** Results are reported as mean  $\pm$  S.E.M. ( $n = 4-8$ ). Student's  $t$  test or repeated measures analysis of variance was used for to determine the statistical significance between control and OLZ groups, as appropriate.  $P < 0.05$  was considered statistically significant.

## Results

### OLZ Administration Increases Weight and Adiposity.

Average body weight at the beginning of the study was  $19.4 \pm 0.1$  g, and did not significantly differ between the groups. All animals gained weight during the course of the study, and there was no mortality or morbidity in any group. OLZ administration did not significantly increase food consumption compared with the animals administered vehicle (control). Despite no apparent increase in food consumption, OLZ administration significantly increased body weight gain by  $\sim 40\%$  over controls (Fig. 1B), similar to what has been observed

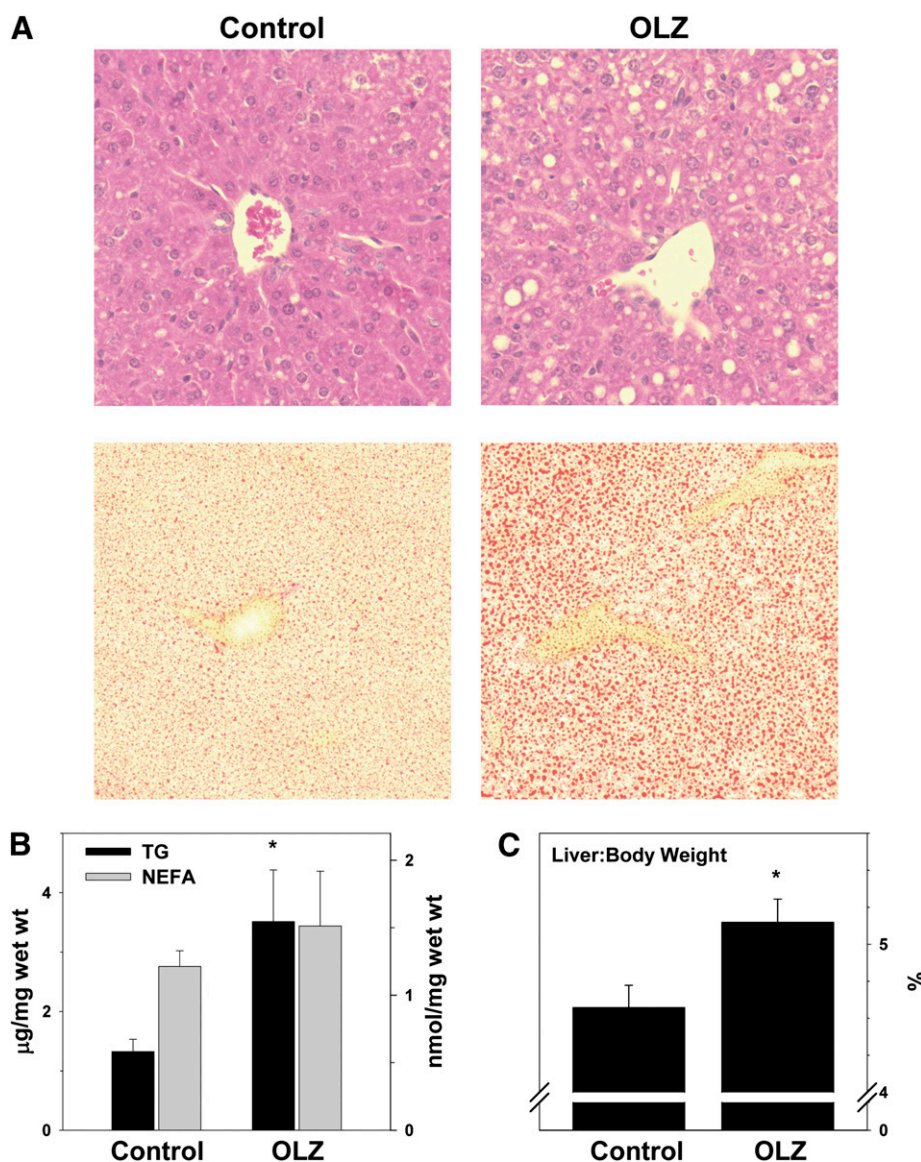


**Fig. 2.** OLZ promotes hepatic lipid accumulation. (A) Representative photomicrographs depicting general histology (H&E; upper panels) and lipid accumulation (Oil Red O; lower panels). (B) Hepatic triglyceride (TG) and nonesterified fatty acid (NEFA) contents. (C) Liver weight measurements taken at sacrifice expressed as a percentage of total body weight. \* $P < 0.05$  compared with controls.

TABLE 1  
Effect of OLZ on plasma variables

Animals and treatments are described under *Materials and Methods*. Data are mean  $\pm$  S.E.M. ( $n = 4-8$ ) and are reported as indicated in the individual rows.

Biochemical Analyses	Control	OLZ
Glucose (mg/dl)	196 $\pm$ 6	329 $\pm$ 13*
Triglycerides (mg/dl)	42 $\pm$ 2	80 $\pm$ 7*
Cholesterol (mg/dl)	50 $\pm$ 6	62 $\pm$ 3
HDL (mg/dl)	34 $\pm$ 4	42 $\pm$ 4
LDL (mg/dl)	8 $\pm$ 2	4 $\pm$ 2
VLDL (mg/dl)	9 $\pm$ 1	16 $\pm$ 1*
ALT (U/l)	33 $\pm$ 9	76 $\pm$ 9*
AST (U/l)	56 $\pm$ 2	80 $\pm$ 6*

ALT, alanine aminotransferase; AST, aspartate aminotransferase; HDL, high-density lipoprotein; LDL, low-density lipoprotein; OLZ, olanzapine; VLDL, very-low-density lipoprotein.

\* $P < 0.05$  compared with controls.

previously by other groups (Cope et al., 2005). An increase in the body fat percentage and gonadal fat pad mass

accompanied the weight gain (Fig. 1, C and D) in OLZ-exposed animals.

**OLZ Promotes Hepatic Lipid Accumulation.** Obesity and/or metabolic syndrome commonly cause lipids to accumulate in the liver (i.e., steatosis). As OLZ administration increased the body weight and total body fat (Fig. 1), the effect of OLZ on hepatic lipid accumulation was determined. A crude index of hepatic lipid accumulation is liver size. OLZ increased liver weight as indicated by the elevation in liver weight to body weight ratio (Fig. 2C). Four weeks of OLZ treatment also increased hepatic fat, as indicated by the presence of macrovesicular and microvesicular lipid droplets in H&E staining (Fig. 2A, top). This effect of OLZ on hepatic lipid accumulation was confirmed by Oil Red O staining (Fig. 2A, bottom).

OLZ administration significantly elevated hepatic TG content  $\sim$ 2-fold. Interestingly, this increase in TG was not coupled with a concomitant increase in hepatic NEFA. This increase in hepatic lipids was paralleled by a statistically

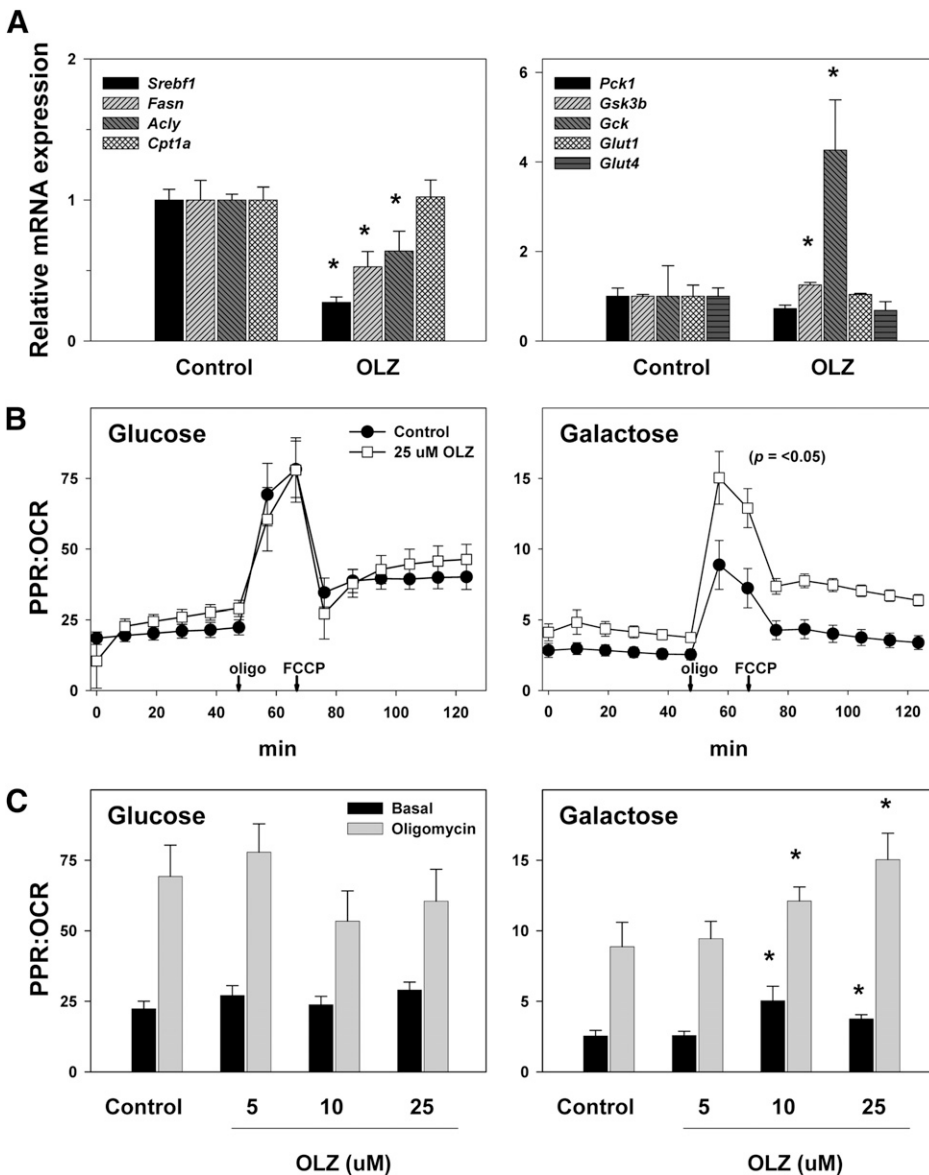


**Fig. 3.** Effects of OLZ on hepatic expression of metabolism-regulating genes and in vitro metabolism of OLZ-treated HepG2 cells. (A) Hepatic mRNA expression of genes for lipid and carbohydrate metabolism determined by quantitative RT-PCR. (B) OCR and PPR rate data (Seahorse) for all time points in HepG2 cells treated with 25  $\mu$ M OLZ or control. (C) Effect of increasing concentrations of OLZ on steady-state PPR/OCR. \* $P < 0.05$  compared with controls.

significant increase in plasma TG and VLDL (Table 1). These effects of OLZ were also accompanied by liver injury, as indicated by significant elevations of plasma alanine aminotransferase (ALT) (~2-fold) and aspartate aminotransferase (AST) (~1.5-fold; Table 1).

**OLZ Modifies Hepatic Expression of Metabolism-Regulating Genes.** Hepatic steatosis is often mediated via direct alterations in the expression of genes key to lipid and carbohydrate metabolism. To further explore the effects of OLZ on hepatic energy metabolism, mRNA expression of genes that are key in regulating the synthesis and catabolism of carbohydrates and lipids was examined by quantitative RT-PCR (Fig. 3A). Four weeks of OLZ administration significantly downregulated the expression of a number of genes involved in lipid biosynthesis, including sterol regulatory element-binding protein 1 (*Srebf1*), fatty acid synthase (*Fasn*), and ATP citrate lyase (*Acly*). Similarly, OLZ exposure upregulated expression of glycogen synthase kinase-3 $\beta$  (*Gsk3b*), a protein that suppresses glycogen synthesis. These changes in expression of anabolism-regulating genes were accompanied by a significant (2.5-fold) increase in expression of glucokinase (*Gck*), a key rate-limiting enzyme in glycolysis. Expression of carnitine palmitoyltransferase 1a (*Cpt1a*), which encodes the rate-limiting enzyme in fatty acid  $\beta$ -oxidation, was unchanged, as were phosphoenolpyruvate carboxykinase 1 (*Pck1*; gluconeogenesis) and glucose transporter type 1 and glucose transporter type 4 (*Glut1* and *Glut4*; basal and insulin-mediated glucose transport, respectively).

**Effects of OLZ on Mitochondrial Respiration.** The mRNA expression data suggest that OLZ administration favors glycolysis (Fig. 3). Previous studies with isolated brain mitochondria have suggested that OLZ partially inhibits mitochondrial respiration [e.g., (Hroudova and Fisar, 2010)]. The effect of OLZ exposure on the balance between glycolysis and mitochondrial respiration was therefore determined in vitro in HepG2 cells by Seahorse in both glucose- and galactose-containing media (see *Materials and Methods*). Under these conditions, the PPR is used as an index of glycolysis, and the OCR is used as an index of mitochondrial function (Fig. 3, B and C). As expected, inhibition of mitochondrial respiration with oligomycin, which forced the cells to rely on anaerobic glycolysis, decreased the rate of OCR while simultaneously increasing the rate of PPR, thereby greatly increasing the PPR/OCR ratio. Uncoupling the mitochondria with FCCP increased the OCR while still maintaining an elevated PPR, causing the PPR/OCR ratio to decrease relative to oligomycin but still remain elevated relative to basal (Fig. 3B). In glucose-containing medium, OLZ had no apparent effect on OCR or PPR at any concentration. When the Warburg/Crabtree effect was overcome by incubating HepG2 cells in galactose-containing media (Warburg et al., 1967), the ratio of PPR/OCR was dramatically decreased, as the cells were forced to rely on oxidative phosphorylation (Marroquin et al., 2007). Under these conditions, OLZ incubation caused a dose-dependent increase in PPR without significantly affecting OCR; these effects of OLZ statistically significantly increased the PPR/OCR ratio (Fig. 3, B and C).

**Effects of OLZ and Glucose and Glycogen Expenditure.** OLZ increased basal (unfasted) plasma glucose, as indicated by plasma taken at sacrifice (Table 1). Previous studies have indicated that OLZ administration may cause insulin resistance and/or glucose intolerance (Coccorello and Moles, 2010). To determine whether OLZ administration

under the current conditions affected glucose tolerance, fasted mice were subjected to the OGTT at 25 days of vehicle or drug administration (see *Materials and Methods*, and Fig. 4A). OLZ did not affect the area under the curve of the OGTT during the testing period. However, OLZ exposure significantly increased the plasma glucose concentrations 15 minutes after bolus gavage (Fig. 4A), although the values were similar to controls at all subsequent time points.

As mentioned earlier, the expression of a key inhibitor of glycogen storage (glycogen synthase kinase-3 $\beta$ ) was statistically significantly increased in livers of OLZ-exposed mice (see Fig. 3A). The effect of OLZ administration on hepatic glycogen storage was therefore assessed by periodic acid-Schiff (PAS) staining (Fig. 4, B and C, representative photomicrographs and quantitative image analysis, respectively). OLZ administration statistically significantly decreased the amount of glycogen stores in unfasted liver by 2-fold compared with controls.

**OLZ Effects on the Hepatic Metabolome, mTOR, and AMPK.** Examining metabolites on an individual basis is time consuming, and the smaller amounts of data produced may unnecessarily narrow the scope of a study. Metabolomic analysis was therefore used to simultaneously characterize several effects of OLZ on liver. Metabolites that varied significantly between the OLZ group and the control group were then analyzed with

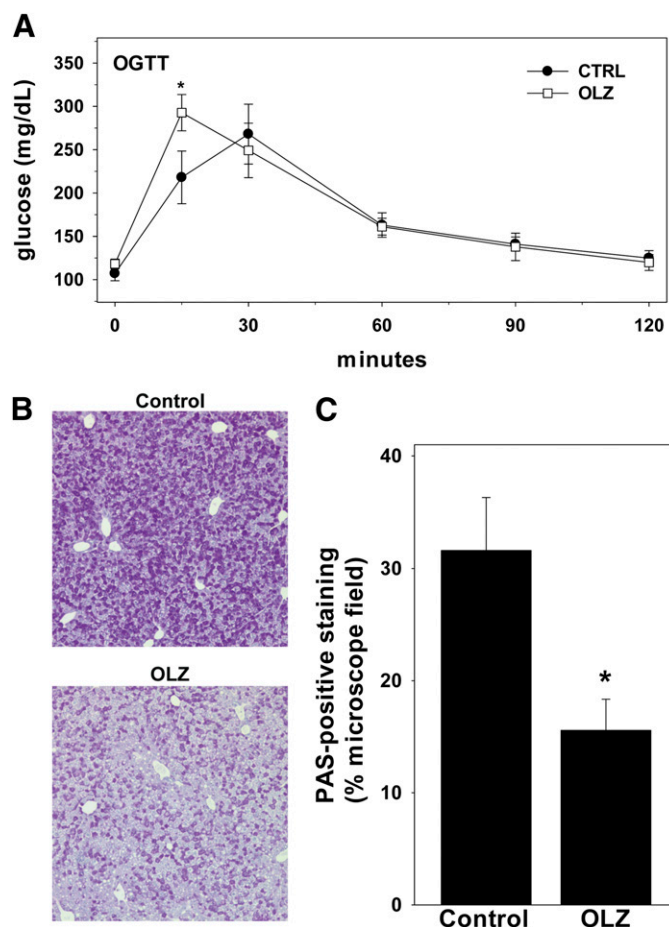
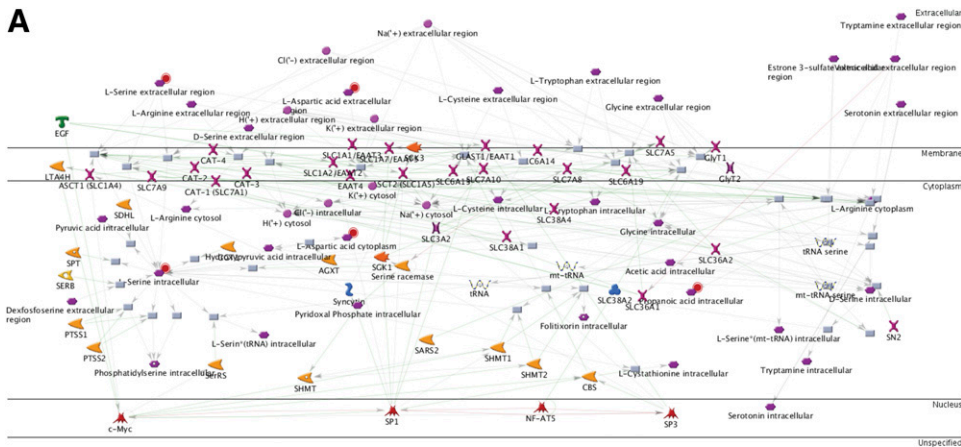


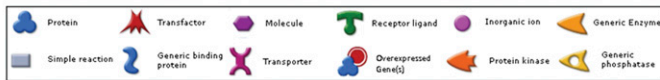
**Fig. 4.** Effects of OLZ and glucose and glycogen expenditure. (A) Effect of OLZ on oral glucose tolerance (OGTT). (B) Representative photomicrographs stained for glycogen content (PAS). (C) Summary of quantitative image-analysis of PAS staining. \* $P < 0.05$  compared with controls by repeated measures analysis of variance (A) or  $t$  test (C).

pathway analysis software, which predicted and mapped the pathways that may be relevant to OLZ treatment (Fig. 5, A and B). Among other findings, amino acids were significantly affected by OLZ: L-glutamine, a putative mediator of mTOR activation (Nicklin et al., 2009), was increased in animals administered OLZ. OLZ also caused a decrease in L-leucine and a parallel increase in L-glutamate, which can act as nitrogen donor and nitrogen acceptor, respectively, in the transamination reaction that regulates the glutamate-glutamine cycle (Islam et al., 2010). Network analysis further predicted the involvement of amino acid transporters Slc7a5 (LAT1) and Slc38a2 (SNAT2), which were recently shown to function as regulators of mTOR signaling, and excitatory amino acid transporter 3 (EAAT3), which is regulated by mTOR activation (Almilaji et al., 2012).

Given the key role of mTOR in mediating carbohydrate and lipid metabolism (Tsang et al., 2007) and the effects of OLZ on these pathways (see Figs. 3–5), the effect of OLZ administration on the activation of mTOR and dependent signaling cascades was determined by Western blot analysis (Fig. 6). OLZ administration increased mTOR activation, as indicated by a statistically significant increase in phosphorylation at Ser248. OLZ administration also increased phosphorylation of p70S6K at Thr389 and 4EBP1 at Thr37/46, indicative of mTORC1 activation (Hara et al., 1997), as well as Akt phosphorylation at Ser473, indicative of mTORC2 activation (Guertin et al., 2006). Interestingly, OLZ treatment also concomitantly increased AMPK activation, as indicated by an increase in phosphorylation at Thr172.



LEGEND



B OLZ compared to CONTROL

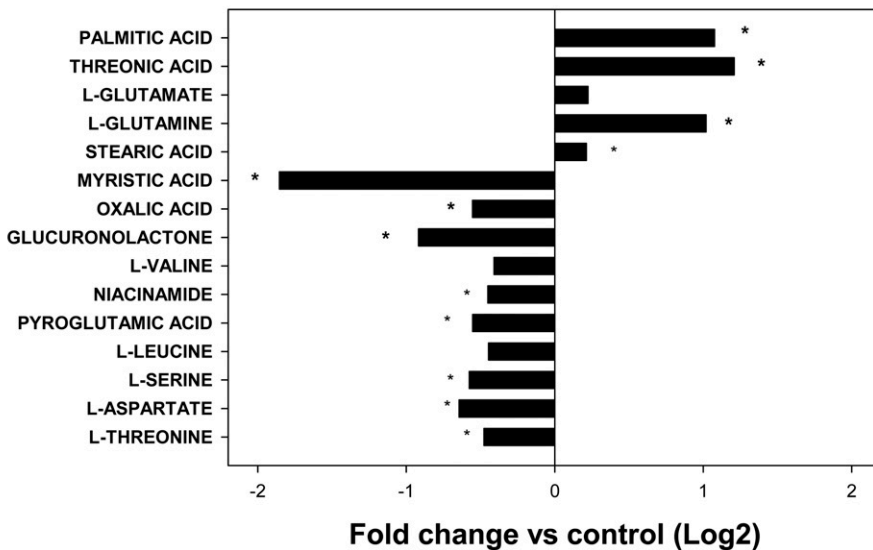
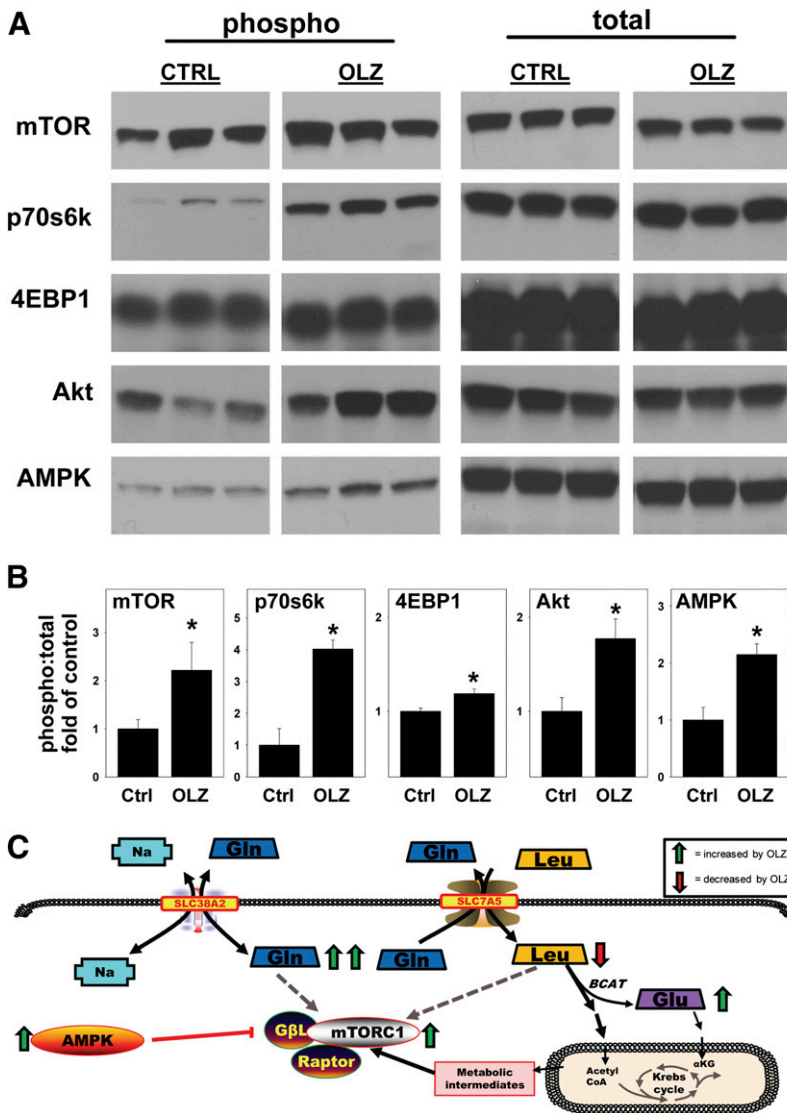


Fig. 5. OLZ effects on hepatic metabolite profile. (A) Metabolites determined by GC×GC-TOF-MS and evaluated with MetaCore software to construct a pathway map. (B) Abundance data for selected metabolites. \**P* < 0.05 compared with controls.



**Fig. 6.** OLZ mediates signaling through mTOR pathways. Liver homogenates were prepared as described under *Materials and Methods*. (A) Representative immunoblots. (B) Ratio of phosphorylated to total protein via quantitative analysis. (C) Proposed mechanisms by which OLZ administration activates mTOR. OLZ promotes flux of glutamine (Gln) and leucine (Leu) through solute carrier 38a2 (SLC38A2 or SNAT2) and solute carrier 7a5 (SLC7A5 or LAT1). Increased concentrations of Gln and Leu induce mTOR signaling. Excess intracellular Leu acts as a nitrogen donor in the branched chain aminotransferase (BCAT) reaction that forms glutamate (Glu). Leu and Glu also contribute metabolic intermediates (e.g., acetyl CoA) to the Krebs cycle. Interestingly, AMPK was simultaneously activated under these conditions (see *Discussion* for additional information). \* $P < 0.05$  compared with controls.

## Discussion

OLZ is an effective drug for treating several psychiatric illnesses and is the drug of choice for schizophrenia and bipolar disorder, but its benefits of OLZ are countered by side effects such as weight gain, glucose intolerance, and dyslipidemia, which impact not only treatment compliance but also increase the health risks to patients. An improved understanding of OLZ actions in the peripheral tissue may therefore identify new approaches to increase the long-term safety and utility of this drug.

As has been observed in other studies, OLZ administration increases body weight and adiposity in mice (Fig. 1). Interestingly, this effect of OLZ was not concurrent with a detectable increase in food consumption (Fig. 1), which suggests that OLZ administration may directly alter energy usage in vivo. In support of this hypothesis, previous experiments have shown that both acute and chronic OLZ administration dysregulates peripheral carbohydrate and lipid metabolism (Chintoh et al., 2008; Coccorello and Moles, 2010; Girault et al., 2012) and directly increases the expression of lipid biosynthetic genes in both liver and adipose tissue (Skrede et al., 2012). In our study,

OLZ administration caused a complex phenotypic alteration in hepatic carbohydrate metabolism. OLZ administration increased glycolysis without an apparent increase in mitochondrial respiration (Figs. 3 and 4) and favored glycogen depletion (Figs. 4 and 6).

OLZ administration also caused a slight but significant increase in glucose intolerance (Fig. 4) and unfasted plasma glucose (Table 1). A shift to an elevated but incomplete (i.e., anaerobic) glycolysis would favor ATP generation from alternate sources such as lipid oxidation. In support of this hypothesis, OLZ administration increases plasma lactic acid levels in humans (Glavina et al., 2011), which is indicative of increased anaerobic glycolysis. Furthermore, OLZ administration lowers the respiratory exchange ratio in rats (Albaugh et al., 2012), which is indicative of a preferential shift to NEFA over carbohydrates as fuel. These results are in line with the observation here that hepatic and plasma triglycerides were elevated by OLZ administration without a commensurate increase in NEFA (Fig. 2; Table 1).

Within the cell, carbohydrate and lipid metabolism are usually under tight control by the protein kinases AMPK and



mTOR. Both AMPK and mTOR are known to act as “sensors” of cellular energy status and to help maintain homeostasis (Hardie, 2007; Guertin and Sabatini, 2009). In general, the downstream effects of AMPK activation are considered catabolic and favor ATP generation during energy depletion. Glycolysis, for example, is enhanced by AMPK. Signaling downstream of AMPK also inhibits ATP-consuming processes (Krause et al., 2002). In contrast to AMPK, mTOR is activated during times of high nutrient availability and favors storage of excess nutrients (e.g., as triglycerides). Activation of the mTOR pathway promotes ATP-consuming processes such as protein and lipid synthesis through its downstream targets p70S6K and 4EBP1.

Previous studies have demonstrated that AMPK is activated in the CNS by OLZ administration (Kim et al., 2007). Furthermore, OLZ increases p70S6K1 and 4EBP1 phosphorylation in cultured hepatocytes, indicative of mTOR activation (Oh et al., 2011). The experiments here demonstrate, for the first time, that OLZ in vivo concomitantly activates AMPK and mTOR pathways in the liver. AMPK and mTOR are generally differentially activated and mediate opposing cellular functions (Kimball, 2006). The outcomes of OLZ administration on hepatic metabolism may reflect these contradictory inputs. These data suggest that treatment with OLZ results in a pseudo-fasted state wherein metabolic resources are abundant but cannot be efficiently used.

The reason for OLZ's concurrent activation of AMPK and mTOR is not immediately clear. Should OLZ indeed induce a pseudo-fasted state, the activation of AMPK may be, in principle, via the “energy sensing” activation of this pathway. As mentioned earlier, OLZ increases peripheral concentrations of glutamate and its metabolites (Fig. 5) (Goff et al., 2002; Yudkoff et al., 2005). The increase in these molecules in the liver may directly activate mTOR (Tato et al., 2011; Laplante and Sabatini, 2012).

Previous studies have indicated that activating AMPK with metformin (a classic approach to treat the metabolic syndrome) confers a disappointingly small beneficial effect against some of the metabolic effects of OLZ (Ehret et al., 2010). This lack of effectiveness may be due to the fact that OLZ administration itself activates AMPK. Alternatively, it has been suggested that “normalizing” mTOR overactivation may be beneficial in obesity and diabetes (Laplante and Sabatini, 2012). It may be that such an approach would be more effective in the context of OLZ administration. The glutamatergic model of mental illness proposes that psychotic disorders are disorders of excitatory amino acid metabolism (Tsai and Coyle, 2002). Therefore, inhibiting mTOR would be arguably downstream of the assumed therapeutic mechanisms of OLZ in psychiatric disorders, and may be a beneficial treatment approach to prevent this drug's metabolic side effects OLZ.

Another important aspect of this work is that OLZ administration significantly increased plasma indices of liver injury in mice (Table 1). Elevation of liver enzymes is described as a common reaction with OLZ administration, and generally results in drug discontinuation (Dominguez-Jimenez et al., 2012). The pathologic changes observed in liver here (Fig. 2) are analogous to those caused by nonalcoholic fatty liver disease (NAFLD). As mentioned earlier, obesity and its sequelae (e.g., NAFLD) have been reaching alarmingly high levels in developed countries. NAFLD is a spectrum of liver diseases, ranging from the relatively benign simple steatosis to active

inflammation, to advanced fibrosis and cirrhosis, and ultimately to hepatocellular carcinoma (Ratziu et al., 2002). Although the prevalence of simple steatosis in individuals at risk for NAFLD can be very high (i.e., >90%), the prevalence of the more severe stages of the disease is much lower (Machado et al., 2006). These factors emphasize that the risk for developing more severe stages of NAFLD is not based solely on obesity or other primary risk factors but rather is mitigated by other factors or “hits” (Day and James, 1998). It is therefore possible that the metabolic effects of OLZ administration could serve as such a second hit in NAFLD.

#### Authorship Contributions

*Participated in research design:* Schmidt, Zhang, Arteil.

*Conducted experiments:* Schmidt, Jokinen, Massey, Falkner, Shi, Yin, Beier.

*Contributed new reagents or analytic tools:* Zhang.

*Performed data analysis:* Schmidt, Zhang, Shi, Yin, Beier, Arteil.

*Wrote or contributed to the writing of the manuscript:* Schmidt, Shi, Zhang, Arteil.

#### References

- Albaugh VL, Vary TC, Ilkayeva O, Wenner BR, Maresca KP, Joyal JL, Breazeale S, Elich TD, Lang CH, and Lynch CJ (2012) Atypical antipsychotics rapidly and inappropriately switch peripheral fuel utilization to lipids, impairing metabolic flexibility in rodents. *Schizophr Bull* **38**:153–166.
- Allison DB, Newcomer JW, Dunn AL, Blumenthal JA, Fabricatore AN, Daumit GL, Cope MB, Riley WT, Vreeland B, and Hibbeln JR, et al. (2009) Obesity among those with mental disorders: a National Institute of Mental Health meeting report. *Am J Prev Med* **36**:341–350.
- Almilaji A, Pakladok T, Guo A, Munoz C, Föller M, and Lang F (2012) Regulation of the glutamate transporter EAAT3 by mammalian target of rapamycin mTOR. *Biochem Biophys Res Commun* **421**:159–163.
- Andrikopoulos S, Blair AR, Deluca N, Fam BC, and Proietto J (2008) Evaluating the glucose tolerance test in mice. *Am J Physiol Endocrinol Metab* **295**:E1323–E1332.
- Bergheim I, Guo L, Davis MA, Lambert JC, Beier JI, Duveau I, Luyendyk JP, Roth RA, and Arteil GE (2006) Metformin prevents alcohol-induced liver injury in the mouse: critical role of plasminogen activator inhibitor-1. *Gastroenterology* **130**:2099–2112.
- Bligh EG and Dyer WJ (1959) A rapid method of total lipid extraction and purification. *Can J Biochem Physiol* **37**:911–917.
- Chintoh AF, Mann SW, Lam L, Lam C, Cohn TA, Fletcher PJ, Nobrega JN, Giacca A, and Remington G (2008) Insulin resistance and decreased glucose-stimulated insulin secretion after acute olanzapine administration. *J Clin Psychopharmacol* **28**:494–499.
- Coccarello R and Moles A (2010) Potential mechanisms of atypical antipsychotic-induced metabolic derangement: clues for understanding obesity and novel drug design. *Pharmacol Ther* **127**:210–251.
- Cope MB, Nagy TR, Fernández JR, Geary N, Casey DE, and Allison DB (2005) Antipsychotic drug-induced weight gain: development of an animal model. *Int J Obes (Lond)* **29**:607–614.
- Day CP and James OF (1998) Steatohepatitis: a tale of two “hits”? *Gastroenterology* **114**:842–845.
- Dominguez-Jiménez JL, Puente-Gutiérrez JJ, Pelado-García EM, Cuesta-Cubillas D, and García-Moreno AM (2012) Liver toxicity due to olanzapine. *Rev Esp Enferm Dig* **104**:617–618.
- Ehret M, Goethe J, Lanosa M, and Coleman CI (2010) The effect of metformin on anthropometrics and insulin resistance in patients receiving atypical antipsychotic agents: a meta-analysis. *J Clin Psychiatry* **71**:1286–1292.
- Girault EM, Alkemade A, Foppen E, Ackermans MT, Fliers E, and Kalsbeek A (2012) Acute peripheral but not central administration of olanzapine induces hyperglycemia associated with hepatic and extra-hepatic insulin resistance. *PLoS ONE* **7**:e43244.
- Glavina T, Mrass D, Dodig T, Glavina G, Pranić S, and Uglešić B (2011) Blood lactate levels in patients receiving first- or second- generation antipsychotics. *Croat Med J* **52**:41–47.
- Goff DC, Hennen J, Lyoo IK, Tsai G, Wald LL, Evins AE, Yurgelun-Todd DA, and Renshaw PF (2002) Modulation of brain and serum glutamatergic concentrations following a switch from conventional neuroleptics to olanzapine. *Biol Psychiatry* **51**:493–497.
- Grayson BE, Seeley RJ, and Sandoval DA (2013) Wired on sugar: the role of the CNS in the regulation of glucose homeostasis. *Nat Rev Neurosci* **14**:24–37.
- Guertin DA and Sabatini DM (2009) The pharmacology of mTOR inhibition. *Sci Signal* **2**:pe24.
- Guertin DA, Stevens DM, Thoreen CC, Burds AA, Kalaany NY, Moffat J, Brown M, Fitzgerald KJ, and Sabatini DM (2006) Ablation in mice of the mTORC components raptor, rictor, or mLST8 reveals that mTORC2 is required for signaling to Akt-FOXO and PKC $\alpha$ , but not S6K1. *Dev Cell* **11**:859–871.
- Hara K, Yonezawa K, Kozłowski MT, Sugimoto T, Andrabi K, Weng QP, Kasuga M, Nishimoto I, and Avruch J (1997) Regulation of eIF-4E BP1 phosphorylation by mTOR. *J Biol Chem* **272**:26457–26463.
- Hardie DG (2007) AMP-activated/SNF1 protein kinases: conserved guardians of cellular energy. *Nat Rev Mol Cell Biol* **8**:774–785.

- Heiskanen T, Niskanen L, Lyytikäinen R, Saarinen PI, and Hintikka J (2003) Metabolic syndrome in patients with schizophrenia. *J Clin Psychiatry* **64**:575–579.
- Hroudova J and Fisar Z (2010) Activities of respiratory chain complexes and citrate synthase influenced by pharmacologically different antidepressants and mood stabilizers. *Neuroendocrinol Lett* **31**:336–342.
- Islam MM, Nautiyal M, Wynn RM, Mobley JA, Chuang DT, and Hutson SM (2010) Branched-chain amino acid metabolon: interaction of glutamate dehydrogenase with the mitochondrial branched-chain aminotransferase (BCATm). *J Biol Chem* **285**:265–276.
- Kapur S, VanderSpek SC, Brownlee BA, and Nobrega JN (2003) Antipsychotic dosing in preclinical models is often unrepresentative of the clinical condition: a suggested solution based on in vivo occupancy. *J Pharmacol Exp Ther* **305**:625–631.
- Kim SF, Huang AS, Snowman AM, Teuscher C, and Snyder SH (2007) From the cover: Antipsychotic drug-induced weight gain mediated by histamine H1 receptor-linked activation of hypothalamic AMP-kinase. *Proc Natl Acad Sci USA* **104**:3456–3459.
- Kimball SR (2006) Interaction between the AMP-activated protein kinase and mTOR signaling pathways. *Med Sci Sports Exerc* **38**:1958–1964.
- Krause U, Bertrand L, and Hue L (2002) Control of p70 ribosomal protein S6 kinase and acetyl-CoA carboxylase by AMP-activated protein kinase and protein phosphatases in isolated hepatocytes. *Eur J Biochem* **269**:3751–3759.
- Laplante M and Sabatini DM (2012) mTOR signaling in growth control and disease. *Cell* **149**:274–293.
- Lee CT, Conde BJ, Mazlan M, Visanuyothin T, Wang A, Wong MM, Walker DJ, Roychowdhury SM, Wang H, and Tran PV (2002) Switching to olanzapine from previous antipsychotics: a regional collaborative multicenter trial assessing 2 switching techniques in Asia Pacific. *J Clin Psychiatry* **63**:569–576.
- Machado M, Marques-Vidal P, and Cortez-Pinto H (2006) Hepatic histology in obese patients undergoing bariatric surgery. *J Hepatol* **45**:600–606.
- Maher AR and Theodore G (2012) Summary of the comparative effectiveness review on off-label use of atypical antipsychotics. *J Manag Care Pharm* **18**(5, Suppl B):S1–S20.
- Marroquin LD, Hynes J, Dykens JA, Jamieson JD, and Will Y (2007) Circumventing the Crabtree effect: replacing media glucose with galactose increases susceptibility of HepG2 cells to mitochondrial toxicants. *Toxicol Sci* **97**:539–547.
- Mathews M and Muzina DJ (2007) Atypical antipsychotics: new drugs, new challenges. *Cleve Clin J Med* **74**:597–606.
- Nicklin P, Bergman P, Zhang B, Triantafellow E, Wang H, Nyfeler B, Yang H, Hild M, Kung C, and Wilson C, et al. (2009) Bidirectional transport of amino acids regulates mTOR and autophagy. *Cell* **136**:521–534.
- Ogden CL, Carroll MD, Curtin LR, McDowell MA, Tabak CJ, and Flegal KM (2006) Prevalence of overweight and obesity in the United States, 1999–2004. *JAMA* **295**:1549–1555.
- Oh KJ, Park J, Lee SY, Hwang I, Kim JB, Park TS, Lee HJ, and Koo SH (2011) Atypical antipsychotic drugs perturb AMPK-dependent regulation of hepatic lipid metabolism. *Am J Physiol Endocrinol Metab* **300**:E624–E632.
- Ratziu V, Bonyhay L, Di Martino V, Charlotte F, Cavallaro L, Sayegh-Tainturier MH, Giral P, Grimaldi A, Opolon P, and Poynard T (2002) Survival, liver failure, and hepatocellular carcinoma in obesity-related cryptogenic cirrhosis. *Hepatology* **35**:1485–1493.
- Sandoval DA, Obici S, and Seeley RJ (2009) Targeting the CNS to treat type 2 diabetes. *Nat Rev Drug Discov* **8**:386–398.
- Skrede S, Fernø J, Vázquez MJ, Fjær S, Pavlin T, Lunder N, Vidal-Puig A, Diéguez C, Berge RK, and López M, et al. (2012) Olanzapine, but not aripiprazole, weight-independently elevates serum triglycerides and activates lipogenic gene expression in female rats. *Int J Neuropsychopharmacol* **15**:163–179.
- Tato I, Bartrons R, Ventura F, and Rosa JL (2011) Amino acids activate mammalian target of rapamycin complex 2 (mTORC2) via PI3K/Akt signaling. *J Biol Chem* **286**:6128–6142.
- Tsai G and Coyle JT (2002) Glutamatergic mechanisms in schizophrenia. *Annu Rev Pharmacol Toxicol* **42**:165–179.
- Tsang CK, Qi H, Liu LF, and Zheng XF (2007) Targeting mammalian target of rapamycin (mTOR) for health and diseases. *Drug Discov Today* **12**:112–124.
- van der Zwaal EM, Luijendijk MCM, Adan RAH, and la Fleur SE (2008) Olanzapine-induced weight gain: chronic infusion using osmotic minipumps does not result in stable plasma levels due to degradation of olanzapine in solution. *Eur J Pharmacol* **585**:130–136.
- Warburg O, Geissler AW, and Lorenz S (1967) Über Wachstum von Krebszellen in Medien, deren Glucose durch Galaktose ersetzt ist. *Hoppe Seylers Z Physiol Chem* **348**:1686–1687.
- Wei X, Shi X, Koo I, Kim S, Schmidt RH, Arteel GE, Watson WH, McClain C, and Zhang X (2013) MetPP: a computational platform for comprehensive two-dimensional gas chromatography time-of-flight mass spectrometry-based metabolomics. *Bioinformatics* **29**:1786–1792.
- Weiden PJ, Maccell JA, and McDonnell DD (2004) Obesity as a risk factor for antipsychotic noncompliance. *Schizophr Res* **66**:51–57.
- Weston-Green K, Huang XF, and Deng C (2012) Alterations to melanocortinergic, GABAergic and cannabinoid neurotransmission associated with olanzapine-induced weight gain. *PLoS ONE* **7**:e33548.
- Yudkoff M, Daikhin Y, Nissim I, Horyn O, Lohovyy B, Lazarow A, and Nissim I (2005) Brain amino acid requirements and toxicity: the example of leucine. *J Nutr* **135**(6, Suppl):1531S–1538S.
- Zhang J, Fang A, Wang B, Kim SH, Bogdanov B, Zhou Z, McClain C, and Zhang X (2011) iMatch: a retention index tool for analysis of gas chromatography-mass spectrometry data. *J Chromatogr A* **1218**:6522–6530.

**Address correspondence to:** Dr. Gavin E. Arteel, Department of Pharmacology and Toxicology, University of Louisville Health Sciences Center, Louisville, KY 40292. E-mail: gavin.arteel@louisville.edu